

## Pharmacokinetics of Paclitaxel-Containing Liposomes in Rats

Submitted: July 30, 2003; Accepted: September 29, 2003; Published: November 21, 2003

Gerald J. Fetterly<sup>1,2</sup> and Robert M. Straubinger<sup>1</sup>

<sup>1</sup>Department of Pharmaceutical Sciences, University at Buffalo, State University of New York, Amherst, NY 14260

<sup>2</sup>Cognigen Corporation, 395 Youngs Road, Buffalo, NY 14221

### ABSTRACT

In animal models, liposomal formulations of paclitaxel possess lower toxicity and equal antitumor efficacy compared with the clinical formulation, Taxol. The goal of this study was to determine the formulation dependence of paclitaxel pharmacokinetics in rats, in order to test the hypothesis that altered biodistribution of paclitaxel modifies the exposure of critical normal tissues. Paclitaxel was administered intravenously in either multilamellar (MLV) liposomes composed of phosphatidylglycerol/phosphatidylcholine (L-pac) or in the Cremophor EL/ethanol vehicle used for the Taxol formulation (Cre-pac). The dose was 40 mg/kg, and the infusion time was 8 to 9 minutes. Animals were killed at various times, and pharmacokinetic parameters were determined from the blood and tissue distribution of paclitaxel. The area under the concentration vs time curve (AUC) for blood was similar for the 2 formulations (L-pac:  $38.1 \pm 3.32$   $\mu\text{g}\cdot\text{h}/\text{mL}$ ; Cre-pac:  $34.5 \pm 0.994$   $\mu\text{g}\cdot\text{h}/\text{mL}$ ), however, the AUC for various tissues was formulation-dependent. For bone marrow, skin, kidney, brain, adipose, and muscle tissue, the AUC was statistically higher for Cre-pac. For spleen, a tissue of the reticuloendothelial system that is important in the clearance of liposomes, the AUC was statistically higher for L-pac. Apparent tissue partition coefficients ( $K_p$ ) also were calculated. For bone marrow, a tissue in which paclitaxel exerts significant toxicity,  $K_p$  was 5-fold greater for paclitaxel in Cre-pac. The data are consistent with paclitaxel release from circulating liposomes, but with efflux delayed sufficiently to retain drug to a greater extent in the central (blood) compartment and reduce penetration into peripheral tissues. These effects may contribute to the reduced toxicity of liposomal formulations of paclitaxel.

**KEYWORDS:** drug delivery, paclitaxel, liposomes, physiological modeling, cancer chemotherapy

### INTRODUCTION

Paclitaxel (as Taxol) has gained widespread use in the treatment of a variety of carcinomas and has become a first line treatment for refractory ovarian, breast, and non-small cell lung cancer.<sup>1-5</sup> Because of poor aqueous solubility, paclitaxel is dissolved for clinical use in dehydrated ethanol and polyethoxylated castor oil (Cremophor EL) in a 1:1 (vol:vol) ratio. Cremophor EL has been shown to cause toxic effects such as life-threatening anaphylaxis.<sup>6-8</sup> High doses of antihistamines and glucocorticoids are administered to manage these adverse effects,<sup>9,10</sup> but these co-administered drugs have raised the possibility of additional pharmacokinetic and pharmacodynamic interactions with paclitaxel. The Cremophor EL vehicle also exerts a range of effects on the biodistribution of the drug,<sup>11-14</sup> modulating multidrug resistance through the P-glycoprotein efflux system and contributing to the nonlinear pharmacokinetics of paclitaxel.

A variety of drug delivery approaches have been investigated to eliminate vehicle toxicity from taxane formulations.<sup>4,15-20</sup> Liposomes have been used to enhance therapeutic effects and reduce the toxicity of a variety of antineoplastic agents.<sup>21-23</sup> Incorporation of paclitaxel in liposomes (L-pac) not only eliminates the hypersensitivity reactions associated with the Cremophor EL vehicle but also decreases the toxicities that arise from the drug's pharmacological action.<sup>4,24-26</sup> A reduction in toxicity to critical normal tissues results in a substantial elevation of the maximum tolerated dose (MTD). The impact of these changes on the therapeutic index are striking; in a paclitaxel-resistant colon tumor model,<sup>4</sup> no dose of paclitaxel in Cremophor EL/ethanol (Cre-pac) had an effect on tumor growth, up to and including high doses that caused delayed (ie, nonvehicle-related) lethality in 100% of the animals. In contrast, L-pac arrested tumor growth and did so at doses that would be lethal to 100% of animals if administered in Cremophor EL.<sup>4</sup> Additional studies in a rat model for

**Corresponding Author:** Robert M. Straubinger, Department of Pharmaceutical Sciences, 539 Cooke Hall, University at Buffalo, State University of New York, Amherst, NY 14260-1200. Tel: (716) 645-2844; Fax: (716) 645-3693; Email: [rms@Buffalo.edu](mailto:rms@Buffalo.edu)

drug-resistant intracranial brain tumors showed substantial tumor growth inhibition and extension of lifespan mediated by L-pac, whereas Cre-pac was ineffective at equivalent doses (R Zhou, RV Mazurchuk, J Tamburlin, and RM Straubinger, unpublished data, 2003.)

The administration regimen appears to exert significant effects on the toxicity of both paclitaxel formulations. L-pac at a cumulative dose of 360 mg/kg was uniformly lethal to mice if administered as 6 doses of 60 mg/kg but was uniformly survived if administered as 9 doses of 40 mg/kg.<sup>4</sup> Similar results were obtained for Cre-pac, but at 30% lower doses.<sup>4</sup> Thus, optimization of drug exposure and dosing regimen appear to play a significant role in the maximization of therapeutic effect and the minimization of toxicity.

The goal of the present study was to compare the bio-distribution kinetics of paclitaxel administered in liposomes or in Cremophor EL. We hypothesize that the blood pharmacokinetics and tissue exposure of paclitaxel can provide insight into the alterations of pharmacology that are observed consistently in therapeutic experiments that compare the efficacy of the 2 paclitaxel formulations.

## MATERIALS AND METHODS

Crystalline paclitaxel was donated by Phytogen Life Sciences (Vancouver, BC, Canada). <sup>3</sup>H-Paclitaxel labeled on the C13 sidechain was obtained from the National Cancer Institute (Bethesda, MD). Cremophor EL was obtained from BASF Corp (Parsippany, NJ). The phospholipids were purchased from Avanti Polar Lipids (Alabaster, AL). Liquid scintillation cocktail was purchased from Packard Instrument Co (Meriden, CT). All organic solvents used for the chromatographic analysis of paclitaxel were high-performance liquid chromatography (HPLC) grade from Fisher Scientific (Pittsburgh, PA).

### *Preparation of Paclitaxel in Cremophor EL*

Approximately 22  $\mu$ Ci of <sup>3</sup>H-paclitaxel in toluene/methanol (specific activity 19.3 Ci/mmol) was added to a glass tube, lyophilized overnight, and stored at 4°C. On the day of drug administration, unlabeled paclitaxel was dissolved in sufficient ethanol to make a 40-mg/mL solution and 0.3 mL was transferred to the tube containing <sup>3</sup>H-paclitaxel; the final specific activity was 1.6 mCi/mmol. An equal volume of Cremophor EL (0.3 mL) was added to produce a stock solution of 20 mg/mL drug. Immediately prior to administration,

the paclitaxel solution was diluted with 0.9% (wt/vol) saline to a final drug concentration of 2 mg/mL.

### *Preparation of Paclitaxel Liposomes*

Paclitaxel liposomes were prepared by a lyophilization method<sup>27</sup> described previously.<sup>17</sup> <sup>3</sup>H-paclitaxel (specific activity 19.3 Ci/mmol) was added to a round-bottomed flask and mixed with sufficient unlabeled paclitaxel in chloroform to produce a final specific activity of 1.6 mCi/mmol. Phosphatidylcholine (PC) and phosphatidylglycerol (PG) were mixed at a 9:1 molar ratio, and paclitaxel was added to a final ratio of 3 mol% with respect to phospholipid. The solution was evaporated at 40°C, dissolved in tert-butanol at a lipid concentration of 100 mM, shell-frozen in liquid nitrogen, and lyophilized overnight. The sample was stored at 4°C until use. For administration, the lyophilized powder was hydrated with 0.9% (wt/vol) saline to produce a final drug concentration of 2 mg/mL (~ 2.34 mM) and a lipid concentration of 78 mM. Liposomal formulations of paclitaxel can be physically unstable above certain drug:lipid ratios.<sup>17,28</sup> The liposomes used here were stable over a time period that greatly exceeded the duration of the experiments. Nonetheless, physical stability and the absence of precipitated drug were verified prior to administration using circular dichroism (CD) and differential interference contrast microscopy assays, which we have described previously.<sup>28-31</sup> The size distribution of the liposome population was determined by quasielastic light scattering (Nicomp 380, PSS-Nicomp, Santa Barbara, CA) using the Nicomp fitting algorithm. A bimodal distribution best fit the data: 59% of the population had a mean diameter of approximately 900 nm (range 630-1400 nm), and 39% had a mean diameter of approximately 200 nm (range 130-250 nm). A minor fraction (2%) had a mean diameter of 26 nm.

### *Pharmacokinetics of Paclitaxel Formulations*

Male Sprague-Dawley rats (200-250 g) were purchased from Harlan Sprague-Dawley (Indianapolis, IN) and acclimated to their surroundings for 1 week. Food and water were provided *ad libitum*. The research protocols were approved in advance by the Institutional Animal Care and Use Committee of the University at Buffalo and conformed to the *Principals of Laboratory Animal Care*.<sup>32</sup>

Cannulas were implanted in the jugular vein under ketamine/xylazine (80/8 mg/kg) anesthesia, and animals were allowed to recover from surgery for 2 to 3 days. Paclitaxel was administered at a dose of 40 mg/kg, which contained approximately 22  $\mu$ Ci of <sup>3</sup>H-paclitaxel. This dose was based on the toxicity and an-

titumor efficacy observed in antitumor experiments with rats bearing drug-resistant intracranial tumors (R Zhou, RV Mazurchuk, J Tamburlin, and RM Straubinger, unpublished data, 2003): 40 mg/kg L-pac was well tolerated upon repetitive dosing and mediated a substantial (26%) increase in median lifespan, whereas the equivalent dose of Cre-pac was more toxic and did not increase survival relative to vehicle-treated controls.

Paclitaxel was infused at a rate of 1 mg/min, equivalent to 0.5 mL/min. Thus, the infusion time was approximately 8 to 9 minutes. At serial time points from 0.2 to 8.2 hours, blood samples were collected in heparinized polypropylene tubes via the jugular vein cannula and frozen at  $-80^{\circ}\text{C}$  until assayed, using 3 to 4 animals per time point. At intervals, some animals were euthanized with methoxyflurane, so that drug levels could be determined in a variety of tissues (ie, bone marrow, spleen, lungs, skin, kidneys, adipose, muscle, brain, and liver). Tissues were collected, weighed, and frozen at  $-80^{\circ}\text{C}$  until assayed. Bone marrow was harvested from femurs using a carefully standardized protocol that involved flushing 1 mL of normal saline through the marrow cavity and collecting the effluent for analysis.

#### **Sample Processing and Analysis of Paclitaxel**

Frozen tissues were crushed into a powder under liquid nitrogen using a mortar and pestle and then homogenized in 9 mL of acetonitrile (ACN). The homogenizer was rinsed with 1 mL ACN to recover residual drug. Samples were placed on ice and clarified by centrifugation for 20 to 30 minutes at 1300g. The supernatants were transferred to 15-mL polypropylene tubes and stored at  $-20^{\circ}\text{C}$ . Blood was processed by adding 10 mL acetonitrile to each 1-mL sample and clarifying by centrifugation for 20 to 30 minutes at 1300g. The supernatant was transferred to 15-mL polypropylene tubes and stored at  $-20^{\circ}\text{C}$ .

Paclitaxel concentration was determined by HPLC analysis using a method described previously.<sup>33</sup> Briefly, the samples were dried under nitrogen gas, reconstituted in 1 mL of methanol, and centrifuged briefly at 15,000g; then a fraction of each sample was injected onto a  $\text{C}_{18}$   $\mu\text{Bondapak}$  column (Waters Inc, Milford, MA) ( $300 \times 3.9$  mm inner diameter [ID], 10  $\mu\text{m}$  particle size) equipped with a  $\mu\text{Bondapak}$  guard column (Waters Inc, Milford, MA) ( $6.6 \times 3.0$  mm ID, 10  $\mu\text{m}$  particle size). The mobile phase was 72% MeOH/28%  $\text{H}_2\text{O}$  and was pumped at a flow rate of 1.0 mL/min. The quantity of  $^3\text{H}$ -paclitaxel was determined using an on-line radioactivity detector (Packard). The use of  $^3\text{H}$ -paclitaxel in conjunction with HPLC separation provided an assay that was both sensitive and spe-

cific for quantifying the active parent compound. The recovery of  $^3\text{H}$ -paclitaxel from blood and various tissues was approximately 90% (data not shown).

#### **Protein Binding**

The fraction of unbound drug was determined using ultrafiltration. Cre-pac or L-pac was added to rat plasma, producing final drug concentrations ranging from 0.05  $\mu\text{g/mL}$  to 0.1 mg/mL. The samples were incubated at  $37^{\circ}\text{C}$  under constant agitation. At various time points from 5 to 120 minutes, 650  $\mu\text{L}$  of the sample was collected. Five hundred microliters was centrifuged in an ultrafiltration device (molecular weight [MW] cutoff 30,000; Amicon, Inc, Beverly, MA) at 1000g for 15 minutes and analyzed for  $^3\text{H}$  using a liquid scintillation analyzer (Packard 1900CA). The free (unbound) fraction of paclitaxel ( $f_u$ ) was calculated as  $f_u = (\text{disintegrations per minute [dpm]/mL ultrafiltrate})/(\text{dpm/mL plasma})$ .

#### **Pharmacokinetic Analysis**

A linear 2-compartment model was used to describe the pharmacokinetics of paclitaxel in both formulations. Drug input was modeled as a short infusion into the central compartment. The rate of change of paclitaxel concentration in the blood and tissue compartments was described by the following equations:

$$V_c \times dC_b / dt = k_0 + CL_d \times (C_t - C_b) - CL_t \times C_b \quad (1)$$

$$V_t \times dC_t / dt = CL_d \times (C_b - C_t) \quad (2)$$

where:  $C_b$  is the blood concentration;  $C_t$  is the tissue drug concentration;  $V_c$  is the central volume of distribution;  $V_t$  is the tissue volume of distribution;  $CL_d$  is the distribution clearance;  $CL_t$  is the total body clearance; and  $k_0$  is the infusion rate. In the case of liposomes, it was not possible to discriminate between drug contained within liposomes and free drug that had been released from liposomes, and for that reason,  $V_t$  and  $CL_d$  should be considered as the "apparent" volume of distribution and distribution clearance, respectively.  $V_c$ ,  $V_t$ ,  $CL_t$ , and  $CL_d$  were calculated by fitting the model to the data using ADAPT II (BMSR, University of Southern California, Los Angeles, CA).<sup>34</sup> The area under the mean paclitaxel concentration-time curves (AUC) and the area under the first moment curve (AUMC) were calculated using the linear trapezoidal rule with extrapolation to infinite time according to the following equations<sup>35</sup>:

$$\text{AUC}_{(0-\infty)} = \int_0^t C dt + C^* / \lambda_z \quad (3)$$

$$\text{AUMC}_{(0-\infty)} = \int_0^t C \times t dt + C^* \times t / \lambda_z + C^* / \lambda_z^2 \quad (4)$$

where  $C^*$  represents the mean drug concentration at the last sampling point ( $t$ ). The elimination rate constant,  $\lambda_z$ , was determined from the terminal slope of the curve. The mean residence time in the body ( $\text{MRT}_B$ ) was calculated as  $\text{MRT}_B = \text{AUMC}/\text{AUC}$ . The apparent steady state volume of distribution ( $V_{ss}$ ) was determined as  $V_{ss} = (\text{MRT}_B - T/2) \times \text{CL}_t$ ,<sup>36</sup> where  $T$  represents the infusion time. The nonsteady-state apparent partition coefficient ( $K_p$ ) was determined as a ratio of  $\text{AUC}_{\text{tissue}}/\text{AUC}_{\text{blood}}$  for noneliminating organs. The  $K_p$  for the liver was calculated by  $K_p = (\text{CL}_{\text{int}} + Q_L)\text{AUC}_L/(Q_L \times \text{AUC}_{\text{blood}})$ ,<sup>37</sup> where  $Q_L$ ,  $\text{AUC}_L$ , and  $\text{CL}_{\text{int}}$  represent the blood flow, paclitaxel AUC, and the intrinsic clearance of paclitaxel for liver, respectively.  $Q_L$  was assumed to be 282 mL/h.<sup>38,39</sup> Yuan's method for bioequivalency studies was used to calculate the SD of the AUCs.<sup>40</sup> The 2 formulations were compared using Student t-test and statistical significance was set at the  $P < 0.05$  level.

### Tissue Distribution

A semiphysiological approach was used to quantify tissue drug concentrations ( $C_t$ ) based on an individual tissue distribution clearance ( $\text{CL}_d$ ) equation:

$$V_t \times dC_t / dt = \text{CL}_d \times (C_b - C_t / K_p) \quad (5)$$

where  $V_t$  is the measured tissue mass and  $K_p$  is the equilibrium tissue: blood partition coefficient of paclitaxel. As described above,  $V_t$  and  $\text{CL}_d$  must be considered "apparent" in the case of liposomes, because liposome-associated drug was not resolved from drug that had been released.

Given that the liver is a major eliminating organ, with intrinsic clearance ( $\text{CL}_{\text{int}}$ ) for paclitaxel, Equation 5 becomes the following:

$$V_L \times dC_L / dt = \text{CL}_d \times (C_b - C_L / K_p) - \text{CL}_{\text{int}} \times C_L / K_p \quad (6)$$

where  $C_L$  is the concentration in the liver. To characterize the tissue data, Equations 5 and 6 were fitted to a physiologically based model using ADAPT II.<sup>34</sup>

## RESULTS

### Pharmacokinetics of Paclitaxel Formulations in Blood

Following a short (8-9 minutes) infusion of 40 mg/kg paclitaxel into rats, the time course of paclitaxel con-

centration in blood was determined for L-pac and Cre-pac formulations (**Figure 1A**). The pharmacokinetic data were best fit by a biexponential model, based on the Akaike Information Criterion, residual variability, and visual inspection of the predicted and observed concentration-time profiles. This model characterized the kinetics of tissue distribution and elimination from the blood as 2 exponential phases. The slope in the elimination phase appeared similar for both formulations (**Figure 1A**), but in the tissue distribution phase (**Figure 1B**), Cre-pac appeared to have a markedly shorter half-life than L-pac.

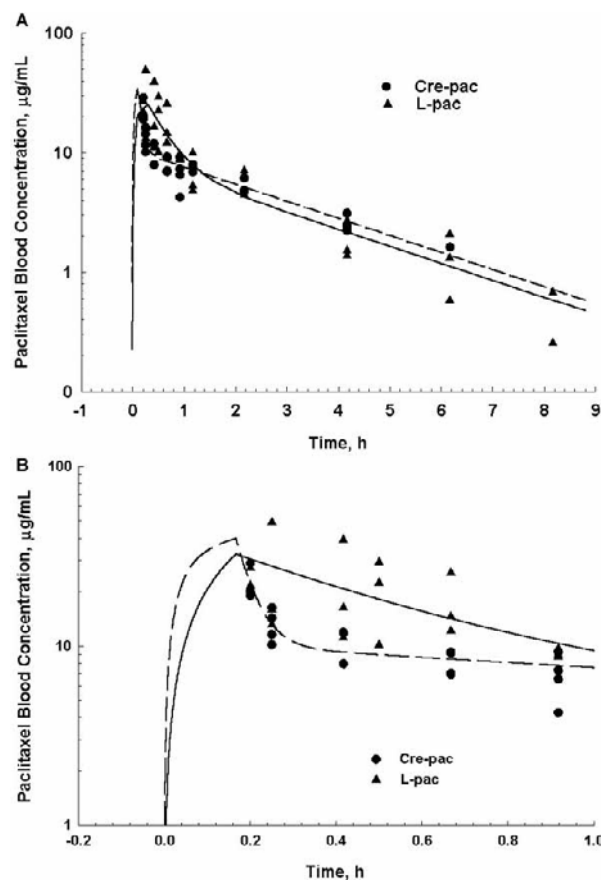


**Figure 1.** Blood concentrations of paclitaxel following a short (8-9 minute) intravenous infusion of 40 mg/kg paclitaxel. Symbols represent the data points, and lines represent the fitting of a 2-compartment linear pharmacokinetic model to the data. Data at each time point consisted of 3 to 4 animals. (A) Filled circles and dashed line: paclitaxel administered in Cre-mophor EL; filled triangles and continuous line: paclitaxel administered in liposomes (3 mol% drug in liposomes composed of PG:PC, 1:9 mol:mol). (B) Details of the blood paclitaxel concentrations during the first hour after administration; lines through the data points were produced by performing a simulation that used the pharmacokinetic model and the model data from Table 1. The lines and symbols are the same as in (A). (Pharmacokinetic model is described in "Materials and Methods" section.)

**Table 1.** Pharmacokinetic Parameters Describing the Disposition of Paclitaxel in Cremophor EL (Cre-paclitaxel) and in Liposomes (L-paclitaxel; 3 mol% drug in PG:PC; 1:9 mol:mol)\*

PK Parameter	L-Paclitaxel		Cre-Paclitaxel	
	Estimate	(% CV)	Estimate	(% CV)
$V_c$ (L/kg)	1.06	(20.4)	0.290	(58.5)
$V_t$ (L/kg)	1.28†	(24.2)	2.62	(7.79)
$V_{ss}$ (L/kg)	2.27		3.27	
$t_{1/2\alpha}$ (h)	0.291	(34.5)	0.0274	(30.3)
$t_{1/2\beta}$ (h)	2.13	(21.0)	2.11	(7.30)
$CL_d$ (L/h/kg)	0.986†	(37.7)	5.70	(30.2)
AUC <sub>(0-6.2 h)</sub> (μg-h/mL)	34.9 ± 1.84		29.6 ± 0.672	
AUC <sub>(0-∞)</sub> (μg-h/mL)	38.1 ± 3.32		34.5 ± 0.994	
$CL_t$ (L/h/kg)	1.07	(8.16)	1.11	(6.52)
MRT (h)	2.20		3.03	

\*AUC indicates area under the concentration vs time curve; CV coefficient of variation; MRT, mean residence time; PC, phosphatidylcholine; PG, phosphatidylglycerol; and PK, pharmacokinetics.

† $V_t$  and  $CL_d$  represent the “apparent tissue” volume of distribution and distribution clearance, respectively, because it was not possible to resolve liposome-associated drug from drug that was released. This “apparent rate” is the aggregate of the free (released) drug  $V_t$  and  $CL_d$  plus the liposome  $V_t$  and  $CL_d$ .  $t_{1/2\alpha}$ , half-life of distribution phase;  $t_{1/2\beta}$ , half-life of elimination phase.

The parameters estimated from the pharmacokinetic analysis are shown in Table 1. The drug exposure profiles (AUC) in the blood were not statistically different for the 2 formulations.  $CL_t$ , mean residence time (MRT), and terminal half-life ( $t_{1/2\beta}$ ) also were similar. In contrast, the  $\alpha$ - (distribution) phase half-life ( $t_{1/2\alpha}$ ), apparent  $V_t$ , and apparent  $CL_d$  differed significantly; for Cre-pac,  $t_{1/2\alpha}$  was approximately 10-fold greater,  $V_t$  was more than 2-fold greater, and  $CL_d$  was more than 6-fold greater than for L-pac (Table 1).  $V_t$  and  $CL_d$  are termed “apparent” because it was not possible to resolve liposome-associated drug from drug that had been released. Therefore, a greater fraction of the total paclitaxel content of blood would reside in liposomes at early times, and this fraction would decline at later times.

### Paclitaxel Binding

Both liposomal and free paclitaxel were approximately 90% bound in plasma. At all time points, the free fraction of drug remained constant as a function of concentration (data not shown). The plasma binding of liposomal paclitaxel was similar to literature values for paclitaxel in Cremophor EL.<sup>41</sup> Red blood cell binding

was assumed to be negligible based on previous studies.<sup>41</sup>

### Biodistribution of Paclitaxel Formulations

The reticuloendothelial system (RES) represents a major mechanism for clearance of circulating liposomes. Therefore, deposition of paclitaxel in liver, lung, and spleen was investigated. L-pac was taken up by the spleen to a greater extent than was Cre-pac; splenic drug concentrations peaked at 70 μg/g for L-pac and at 12 μg/g for Cre-pac (**Figure 2A**). In the lungs, the drug concentration peaked at 40 μg/g for L-pac and at 10 μg/g for Cre-pac (**Figure 2B**), and the higher drug levels achieved with L-pac persisted for approximately 2.5 to 3 hours. Subsequently, lung levels declined more quickly for L-pac than for Cre-pac, suggesting that a substantial portion of the liposome-deposited lung dose was not in the free (released) form. In the liver, drug concentrations were similar for both formulations, with peak levels of approximately 10 μg/g (**Figure 2C**).

Other tissues were evaluated for exposure to paclitaxel. Skin, kidneys, adipose, muscle, brain, and bone marrow showed a greater tissue exposure for Cre-pac

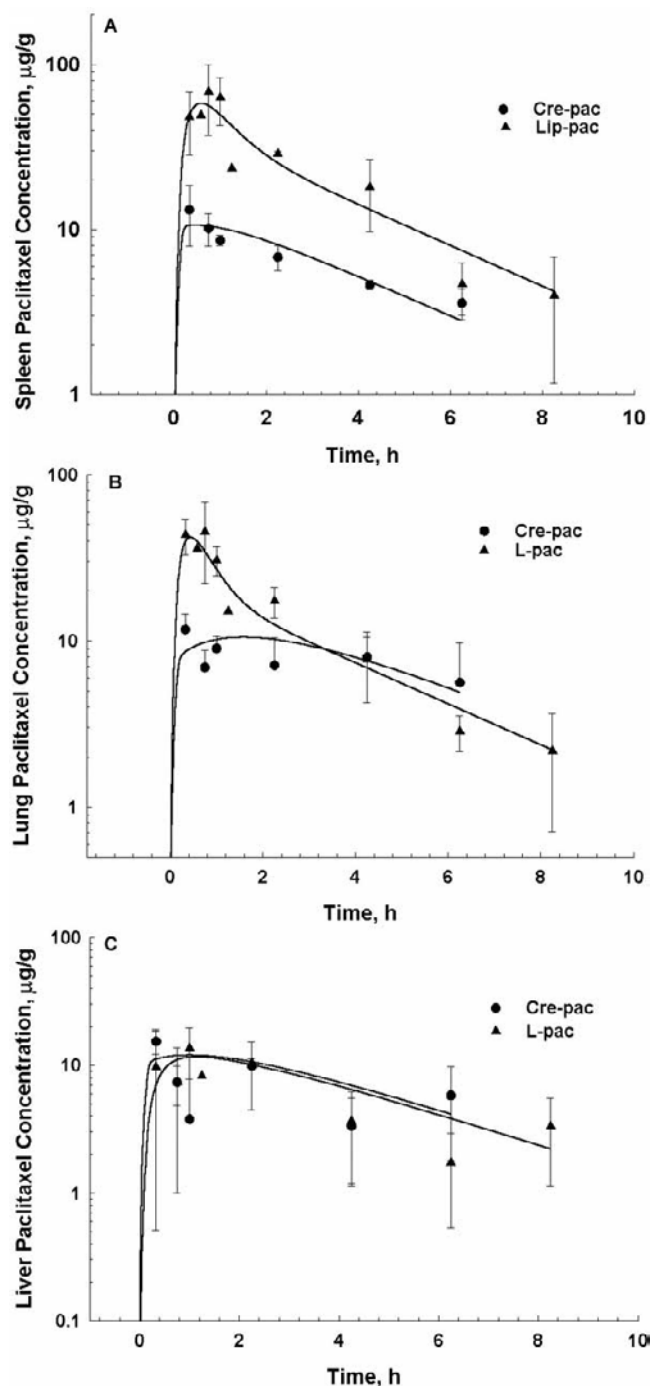


**Figure 2.** Exposure of the (A) spleen, (B) lungs, and (C) liver to paclitaxel. Filled triangles: paclitaxel in liposomes (3 mol% drug in liposomes of PG:PC; 1:9 mol:mol); filled circles: paclitaxel in Cremophor EL. Data represent the mean  $\pm$  SD of 3 to 4 animals.

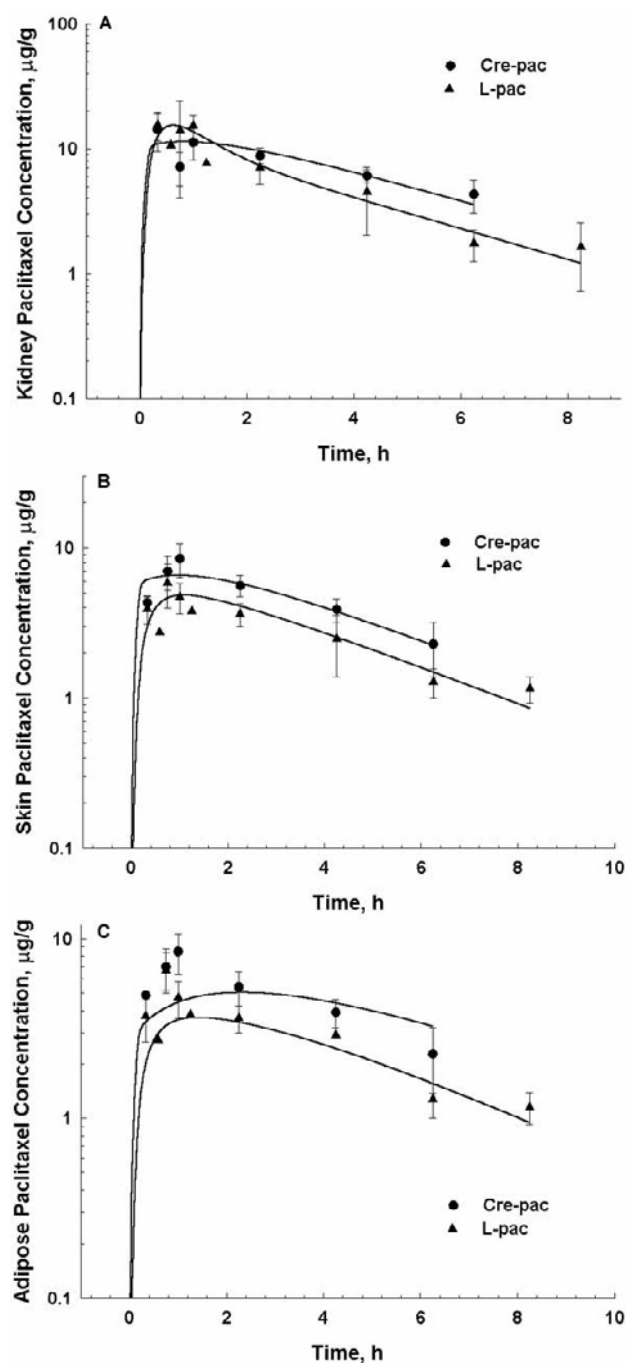


**Figure 3.** Exposure of the (A) kidneys, (B) skin, and (C) adipose tissue to paclitaxel. Filled triangles: paclitaxel in liposomes (3 mol% drug in liposomes of PG:PC; 1:9 mol:mol); filled circles: paclitaxel in Cremophor EL. Data represent the mean  $\pm$  SD of 3 to 4 animals.

(Figures 3 and 4). In all of these tissues, drug followed a monoexponential decline in concentration over time for both formulations. In the kidneys, the paclitaxel

concentration peaked at approximately 20 µg/g (Figure 3A). Drug concentrations in the skin, adipose, and muscle ranged from 5 to 10 µg/g and peaked at 1 hour

after paclitaxel administration (**Figures 3B, 3C, and 4A**). The peak concentration of paclitaxel in the brain was only 1  $\mu\text{g/g}$  (**Figure 4B**). Peak concentrations of paclitaxel in bone marrow ranged from 0.1 to 1  $\mu\text{g/mL}$  (**Figure 4C**) and were similar for both formulations. Drug concentrations could not be determined reliably in intestinal tissues, owing to a variable, inconsistent contribution of drug from the feces.

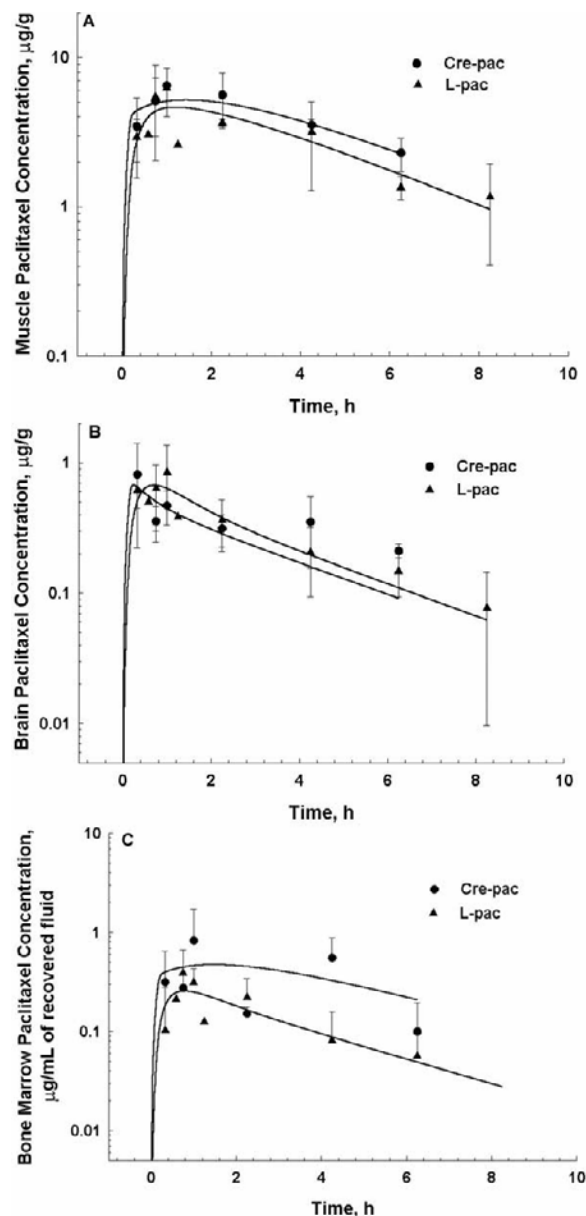


**Figure 4.** Exposure of the (A) muscle, (B) brain, and (C) bone marrow to paclitaxel. Filled triangles: paclitaxel in liposomes (3 mol% drug in liposomes of PG:PC; 1:9 mol:mol); filled circles: paclitaxel in Cremophor EL. Data represent the mean  $\pm$  SD of 3 to 4 animals.

Assay sensitivity and selectivity permitted quantification of L-pac for 8 hours postadministration and of Cre-pac for 6 hours; the pharmacokinetic profiles of both formulations in each tissue captured more than 85% of the total AUC. Thus, total drug exposure (AUC) in the blood and various tissues could be compared for both formulations (**Figure 5**). Although the AUC for blood was similar, the tissue distribution was higher for Cre-pac ( $P < 0.05$ ) in all tissues except the spleen, which represents a major organ of the RES system.

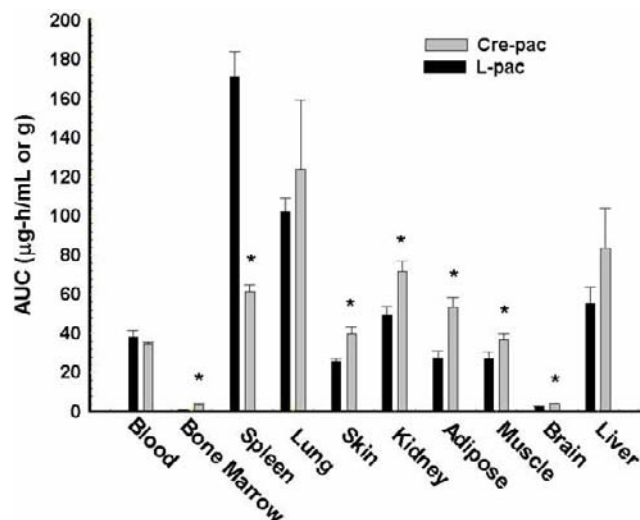


**Figure 5.** Comparative tissue distribution (AUC) of paclitaxel formulations. Filled bars: liposomal formulation (3 mol% drug in liposomes of PG:PC; 1:9 mol:mol); open bars: Cremophor EL formulation. Data represent the mean  $\pm$  SD; paired t-test,  $< 0.05$ .

Individual drug distribution clearances ( $CL_d$ ) and apparent partition coefficients ( $K_p$ ) were calculated using the ratio of the AUC values for the tissues and fitting of the data to a physiologically based model (**Table 2**). The data for drug concentration in all assayed tissues was fit simultaneously, and the predicted values for  $K_p$  were similar to those calculated from experimental data (**Table 2**).

For the spleen,  $K_p$  was 1.77 for Cre-pac and 4.48 for L-pac, while  $CL_d$  was 1.00 mL/h for Cre-pac and 6.41 mL/h for L-pac. In contrast,  $K_p$  for bone marrow was 0.1 for Cre-pac and 0.0241 for L-pac. A reliable estimation of  $CL_d$  for Cre-pac in the bone marrow was not obtained because of variability in the bone marrow data and in the simultaneous fitting of the 18 equations that comprised the physiologically based pharmacokinetic model.  $K_p$  for the skin, kidneys, muscle, and brain were approximately 1.5- to 2-fold greater for Cre-pac than for L-pac, suggesting preferential uptake of paclitaxel

**Table 2.** Apparent Tissue Partition Coefficients and Individual Distribution Clearances Were Determined for Liposomal Paclitaxel and Paclitaxel in Cremophor EL/Ethanol\*

Tissue	Formulation	$K_p$ (Calculated)	$K_p$ (Estimated)	$CL_d$ (mL/h) (Estimated)
Spleen	L-pac	4.48	4.45	6.41
	Cre-pac	1.77	1.4	1
Lung	L-pac	2.68	2.49	17.4
	Cre-pac	3.59	1.93	2.02
Skin	L-pac	0.668	0.645	23.5
	Cre-pac	1.15	1.01	39.7
Kidney	L-pac	1.29	1.25	5.67
	Cre-pac	2.07	1.67	3.59
Heart	L-pac	0.976	1.01	6.36
	Cre-pac	1.51	1.39	2.3
Adipose	L-pac	0.719	0.588	7.7
	Cre-pac	1.54	1.14	10.2
Muscle	L-pac	0.709	0.671	51.3
	Cre-pac	1.06	0.917	66.1
Brain	L-pac	0.0658	0.061	0.16
	Cre-pac	0.113	0.054	0.189
Liver	L-pac	2.14	11.9	12.1
	Cre-pac	3.64	5.71	15.8
Bone Marrow	L-pac	0.0241	0.026	0.39
	Cre-pac	0.1	0.084	$1.14 \times 10^{-8}$

\* $CL_d$  indicates distribution clearance;  $K_p$ , partition coefficient; L-pac, liposomal paclitaxel; and Cre-pac, paclitaxel in Cremophor EL.

in Cremophor EL in these tissues. The partition coefficients for lung and liver also indicated a trend toward greater uptake of Cre-pac by these organs, but the values were not statistically different for the 2 formulations.

## DISCUSSION

Liposomes provide a formulation alternative for the administration of paclitaxel and can confer beneficial effects on the pharmacology and toxicology of the drug. These formulations not only eliminate the acute toxicity of the Cremophor EL vehicle but also alter the efficacy of the drug. Incorporation of paclitaxel in liposomes reduced drug toxicity in both drug-sensitive and drug-resistant animal models.<sup>4,24-26,42</sup> In paclitaxel-resistant rodent models of colon carcinoma<sup>4</sup> and brain tumors,<sup>43</sup> tumor growth was suppressed more effectively by drug in liposomes, and the maximal response

was observed at doses that were more toxic or exceeded the MTD if administered in Cremophor EL. It was also observed for both formulations that changes in the treatment regimen markedly altered mortality, indicating the role that pharmacokinetics plays in the efficacy and toxicity of therapy.

In a drug-sensitive murine xenograft model employing the human ovarian carcinoma line A121a, both paclitaxel and docetaxel in liposomes were equipotent with the equivalent free drug administered in its clinically used vehicle.<sup>25</sup> In the highly drug-resistant murine Colon-26 model, paclitaxel in liposomes equaled or exceeded slightly the gram-per-gram antitumor potency of paclitaxel in Cremophor EL. Of interest, the antitumor effect of paclitaxel liposomes did not vary significantly for liposomes of widely varying properties (eg, long- vs short-circulation time).<sup>4</sup> In the moderately drug-resistant intracranial 9L rat brain tumor model, liposomal incorporation increased significantly the an-



titumor potency of paclitaxel (R Zhou, RV Mazurchuk, J Tamburlin, and RM Straubinger, unpublished data, 2003). Thus, both drug toxicity and antitumor potency are sensitive to formulation characteristics and pharmacokinetic properties.

In this study, we investigated the formulation-dependent pharmacokinetics of paclitaxel in blood and the deposition in key tissues. The results show, with several important exceptions, that the blood pharmacokinetics of paclitaxel are similar for drug administered in liposomes or in Cremophor EL. The findings support the hypothesis that drug is released from circulating liposomes, but release is retarded sufficiently to alter critical pharmacodynamic parameters that may underlie dose-limiting toxicities.

A disadvantage of measuring whole-blood drug levels is that liposome-incorporated drug cannot be distinguished from released drug, and released drug could consist of free-, protein-bound-, and cell-associated fractions. Although it has been possible to measure liposomal release rates in blood for several drugs,<sup>44,45</sup> these methods are not suitable for paclitaxel. The drug is very low in aqueous solubility, highly hydrophobic, and, in contact with biological media, may be exchangeable with serum proteins because of its orientation in the phospholipid bilayer. However, this aggregate measure of drug distribution does not confound interpretation. The distribution of the drug between the protein-bound and free fractions is well characterized (generally ~95% bound), and blood cell uptake of paclitaxel is low.<sup>11,41,46</sup> Drug released from circulating liposomes should bind rapidly to serum proteins and subsequently be subject to the same pharmacokinetic processes and fate as "free" drug administered in the Cremophor EL-based vehicle.

In the present study, encapsulation of paclitaxel at 3 mol% in PC:PG (9:1 mol:mol) liposomes of 0.2 to 0.9  $\mu$ m diameter altered drug exposure ( $C \times t$ ) in the blood and various tissues. For both formulations, terminal half-lives ( $t_{1/2\beta}$ ), total drug exposure (AUC) in the blood, and total body clearances ( $CL_t$ ) were similar (**Table 1**). However, the tissue volume of distribution,  $V_t$  (1.28 L/kg for L-pac compared with 2.62 L/kg for Cre-pac), and the distribution clearance,  $CL_d$  (0.986 L/h/kg for L-pac and 5.70 L/h/kg for Cre-pac; **Figure 1, Table 1**), were altered significantly, suggesting that the kinetics of drug transfer from the central compartment to the peripheral tissue compartment is delayed for liposomal formulations, (ie, release of paclitaxel from liposomes is not instantaneous upon administration.) This modulation of drug release rate by liposomes appears to impact paclitaxel tissue distribution

and may explain formulation-dependent differences in toxicity and antitumor efficacy.

The tissues of the reticuloendothelial system (liver, spleen, and lung) comprise the major route of clearance for circulating liposomes. Therefore, one would expect drug deposition in the RES tissues to be significantly greater for L-pac than for Cre-pac. However, no statistically significant formulation-dependent differences were observed in the liver exposure profile. This finding may be rationalized by the fact that free drug (as Cre-pac) is cleared rapidly by hepatocytes and metabolized extensively in the liver, whereas liposomes are taken up avidly by Kupffer cells. Thus, formulation-dependent differences may exist in the liver in terms of clearance mechanisms and drug distribution at the cellular level. However, if these distinct clearance mechanisms have similarly high rates, liver exposure profiles will be similar for the 2 formulations.

Peak concentrations were higher for L-pac than for Cre-pac in spleen and lung, consistent with their role in RES-mediated clearance of liposomes. This rapid sequestration of drug (**Figure 2, Table 2**) was followed by a more rapid clearance than observed for drug administered as Cre-pac. Because neither spleen nor lung likely plays a significant role in the elimination of paclitaxel, drug is probably cleared by remobilization. The very rapid decline of L-pac levels observed in lung suggests that the remobilized drug may not yet have been released entirely from liposomes. Thus sequestration and rerelease of liposome-delivered drug from tissue depots may comprise a second mechanism of paclitaxel biodistribution that is both plausible and consistent with our data. RES tissues may act as a reservoir for encapsulated drug, and cell-mediated liposome processing<sup>47</sup> or interaction of liposomes with nonspecific proteins could release paclitaxel for redistribution to other tissues. The application of a physiological pharmacokinetic model to the data revealed 2 distinct pharmacokinetic phases in the spleen and lung, consistent with multiple clearance mechanisms.

A slower rate of accumulation of paclitaxel in non-RES tissues was observed for L-pac (Figures 3 and 4). In skin, muscle, and adipose tissue, peak concentrations were observed approximately 1 hour following administration. These profiles suggest that drug continued to accumulate in non-RES tissues in parallel with drug clearance from the central compartment, as might be expected for drug rereleased from tissue depots.

Considering the formulation-dependent differences in the distribution phase of the blood concentration-time profiles, along with differences in tissue penetration and apparent volume of distribution, the data are con-

sistent with delayed release of paclitaxel from liposomes. However, drug-release rates likely are much greater than for other liposomal formulations, such as the sterically-stabilized doxorubicin liposomes,<sup>23,48,49</sup> which have recently received clinical approval (Doxil or Caelyx; Alza, Inc, Mountain View, CA); semi-precipitation of the doxorubicin within the polyethylene-glycol-coated liposome particle results in a highly stable formulation, for which tissue deposition of the drug reflects deposition of the liposome carrier.<sup>23,44,50,51</sup>

In spite of a release rate for paclitaxel that may be much higher than for doxorubicin in sterically stabilized liposomes, incorporation of paclitaxel in liposomes alters toxicity and antitumor effect in a beneficial manner, and the observed pharmacokinetics suggest mechanisms by which the reduction in toxicity may occur.

Overall, the initial extensive RES uptake of liposomal paclitaxel, coupled with noninstantaneous release of drug from circulating liposomes, may limit the systemic exposure of non-RES tissues to paclitaxel (**Table 2**). These effects may initially confine a greater fraction of drug to the central compartment, thus reducing the peak concentrations to which critical normal tissues are exposed. The subsequent release of liposomal drug from the RES could provide a slower, sustained tissue distribution rate and lower tissue volume of distribution after administration of the liposomal drug. These effects may exert not only a direct effect on dose-limiting toxicity but also may underlie the preservation or enhancement of antitumor efficacy observed following administration of liposomal paclitaxel.

## ACKNOWLEDGEMENTS

This work was supported by a research grant CA-55251 from the National Cancer Institute, National Institutes of Health, Bethesda, MD (Robert M Straubinger) and a predoctoral fellowship from the Pharmaceutical Research and Manufacturers of America (PhRMA), Washington, DC (Gerald J. Fetterly). The authors thank Dr Rusty Arnold and Jeanine Slack for helpful discussions and comments.

## REFERENCES

- Guastalla JP, Lhomme C, Dauplat J, et al. Taxol (paclitaxel) safety in patients with platinum pretreated ovarian carcinoma: an interim analysis of a Phase II multicenter study. *Ann Oncol*. 1994;5(suppl 6):S33-38.
- Kubota T, Matsuzaki SW, Hoshiya Y, et al. Antitumor activity of paclitaxel against human breast carcinoma xenografts serially transplanted into nude mice. *J Surg Oncol*. 1997;64:115-121.
- Adler LM, Herzog TJ, Williams S, Rader JS, Mutch DG. Analysis of exposure times and dose escalation of paclitaxel in ovarian cancer cell lines. *Cancer*. 1994;74:1891-1898.
- Sharma A, Mayhew E, Straubinger RM. Antitumor effect of taxol-containing liposomes in a taxol-resistant murine tumor model. *Cancer Res*. 1993;53:5877-5881.
- Murphy WK, Fossella FV, Winn RJ, et al. Phase II study of taxol in patients with untreated advanced non-small-cell lung cancer. *J Natl Cancer Inst*. 1993;85:384-388.
- Weiss RB, Donehower RC, Wiernik PH, et al. Hypersensitivity reactions from taxol. *J Clin Oncol*. 1990;8:1263-1268.
- Szebeni J, Muggia FM, Alving CR. Complement activation by Cremophor EL as a possible contributor to hypersensitivity to paclitaxel: an in vitro study. *J Natl Cancer Inst*. 1998;90:300-306.
- van Zuylen L, Karlsson MO, Verweij J, et al. Pharmacokinetic modeling of paclitaxel encapsulation in Cremophor EL micelles. *Cancer Chemother Pharmacol*. 2001;47:309-318.
- Bookman MA, Kloth DD, Kover PE, Smolinski S, Ozols RF. Short-course intravenous prophylaxis for paclitaxel-related hypersensitivity reactions. *Ann Oncol*. 1997;8:611-614.
- Jamis-Dow CA, Klecker RW, Katki AG, Collins JM. Metabolism of taxol by human and rat liver in vitro: a screen for drug interactions and interspecies differences. *Cancer Chemother Pharmacol*. 1995;36:107-114.
- Sparreboom A, van Zuylen L, Brouwer E, et al. Cremophor EL-mediated alteration of paclitaxel distribution in human blood: clinical pharmacokinetic implications. *Cancer Res*. 1999;59:1454-1457.
- Ellis AG, Webster LK. Inhibition of paclitaxel elimination in the isolated perfused rat liver by Cremophor EL. *Cancer Chemother Pharmacol*. 1999;43:13-18.
- Sparreboom A, Verweij J, van der Burg ME, et al. Disposition of Cremophor EL in humans limits the potential for modulation of the multidrug resistance phenotype in vivo. *Clin Cancer Res*. 1998;4:1937-1942.
- van Tellingen O, Huizing MT, Panday VR, et al. Cremophor EL causes (pseudo-) non-linear pharmacokinetics of paclitaxel in patients. *Br J Cancer*. 1999;81:330-335.
- Bartoli MH, Boitard M, Fessi H, et al. In vitro and in vivo antitumoral activity of free and encapsulated taxol. *J Microencap*. 1990;7:191-197.
- Straubinger RM, Sharma A, Murray M, Mayhew E. Novel taxol formulations: Taxol-containing liposomes. *J Natl Cancer Inst Monogr*. 1993;(15):69-78.
- Sharma A, Straubinger RM. Novel taxol formulations: preparation and characterization of taxol-containing liposomes. *Pharm Res*. 1994;11:889-896.
- Alkan-Onyuksel H, Ramakrishnan S, Chai HB, Pezzuto JM. A mixed micellar formulation suitable for the parenteral administration of taxol. *Pharm Res*. 1994;11:206-212.
- Sharma D, Chelvi TP, Kaur J, et al. Novel Taxol formulation: polyvinylpyrrolidone nanoparticle-encapsulated Taxol for drug delivery in cancer therapy. *Oncol Res*. 1996;8:281-286.
- Scialli AR, Waterhouse TB, Desesso JM, Rahman A, Goeringer GC. Protective effect of liposome encapsulation on paclitaxel developmental toxicity in the rat. *Teratology*. 1997;56:305-310.
- Papahadjopoulos D, Allen T, Gabizon A, et al. Sterically-stabilized liposomes: improvements in pharmacokinetics and antitumor therapeutic efficacy. *Proc Natl Acad Sci U S A*. 1991;88:11460-11464.

22. Drummond DC, Meyer O, Hong K, Kirpotin DB, Papahadjopoulos D. Optimizing liposomes for delivery of chemotherapeutic agents to solid tumors. *Pharmacol Rev.* 1999;51:691-743.
23. Mayer LD, Tai LCL, Ko DSC, et al. Influence of vesicle size, lipid composition, and drug-to-lipid ratio on the biological activity of liposomal doxorubicin in mice. *Cancer Res.* 1989;49:5922-5930.
24. Sharma A, Sharma US, Straubinger RM. Paclitaxel-liposomes for intracavitary therapy of intraperitoneal P388 leukemia. *Cancer Lett.* 1996;107:265-272.
25. Sharma A, Straubinger RM, Ojima I, Bernacki RJ. Antitumor efficacy of taxane liposomes on a human ovarian tumor xenograft in nude athymic mice. *J Pharm Sci.* 1995;84(12):1400-1404.
26. Cabanes A, Briggs KE, Gokhale PC, Treat JA, Rahman A. Comparative in vivo studies with paclitaxel and liposome-encapsulated paclitaxel. *Int J Oncol.* 1998;12:1035-1040.
27. Perez-Soler R, Lopez-Berestein G, Lautersztain J, et al. Phase I clinical and pharmacological study of liposome-entrapped cis-bis-neodecanoato-trans-R,R-1,2-diaminocyclohexane platinum(II). *Cancer Res.* 1990;50:4254-4259.
28. Campbell RB, Balasubramanian SV, Straubinger RM. Influence of cationic lipids on the stability and membrane properties of paclitaxel-containing liposomes. *J Pharm Sci.* 2001;90(8):1091-1105.
29. Balasubramanian SV, Alderfer JL, Straubinger RM. Solvent- and concentration-dependent molecular interactions of taxol (paclitaxel). *J Pharm Sci.* 1994;83(10):1470-1476.
30. Balasubramanian SV, Straubinger RM. Taxol-lipid interactions: taxol-dependent effects on the physical properties of model membranes. *Biochemistry.* 1994;33:8941-8947.
31. Sharma US, Balasubramanian SV, Straubinger RM. Pharmaceutical and physical properties of paclitaxel (Taxol) complexes with cyclodextrins. *J Pharm Sci.* 1995;84(10):1223-1230.
32. National Institutes of Health. *Principals of Laboratory Animal Care.* Bethesda, MD: National Institutes of Health. Revised 1985. Publication No. 85-23.
33. Sharma A, Conway WD, Straubinger RM. Reversed-phase high-performance liquid chromatographic determination of taxol in mouse plasma. *J Chromatogr B.* 1994;655:315-319.
34. D'Argenio DZ, Schumitzky A. A program package for simulation and parameter estimation in pharmacokinetic systems. *Comput Meth Prog Biomed.* 1979;9:115-134.
35. Yamaoka K, Nakagawa T, Uno T. Statistical moments in pharmacokinetics. *J Pharmacokinet Biopharm.* 1978;6:547-558.
36. Benet L, Galeazzi RL. Noncompartmental determination of the steady-state volume of distribution. *J Pharm Sci.* 1979;68(8):1071-1074.
37. Gallo JM., Lam FC, Perrier DG. Area method for the estimation of partition coefficients for physiological pharmacokinetic models. *J Pharmacokinet Biopharm.* 1987;15:271-280.
38. Gerlowski LE, Jain RK. Physiologically based pharmacokinetic modeling: principles and applications. *J Pharm Sci.* 1983;72:1103-1127.
39. Mordenti J. Man versus beast: pharmacokinetic scaling in mammals. *J Pharm Sci.* 1986;75:1028-1040.
40. Yuan J. Estimation of variance for AUC in animal studies. *J Pharm Sci.* 1993;82:761-763.
41. Kumar GN, Walle UK, Bhalla KN, Walle T. Binding of Taxol to human plasma, albumin, and  $\alpha$ 1-acid glycoprotein. *Res Commun Chem Pathol Pharmacol.* 1993;80:337-344.
42. Sharma A, Mayhew E, Bolcsak L, et al. Activity of paclitaxel liposome formulations against human ovarian tumor xenografts. *Int J Cancer.* 1997;71:103-107.
43. Zhang X, Burt HM, Mangold G, et al. Anti-tumor efficacy and biodistribution of intravenous polymeric micellar paclitaxel. *Anti-cancer Drugs.* 1997;8:696-701.
44. Gabizon A, Shiotar R, Papahadjopoulos D. Pharmacokinetics and tissue distribution of doxorubicin encapsulated in stable liposomes with long circulation times. *J Natl Cancer Inst.* 1989;81:1484-1488.
45. Chonn A, Semple S, Cullis P. Separation of large unilamellar liposomes from blood components by a spin column procedure: towards identifying plasma proteins which mediate liposome clearance in vivo. *Biochim Biophys Acta.* 1991;1070:215-222.
46. Sparreboom A, van Tellingen O, Nooijen WJ, Beijnen JH. Tissue distribution, metabolism and excretion of paclitaxel in mice. *Anticancer Drugs.* 1996;7:78-86.
47. Straubinger RM, Hong K, Friend DS, Papahadjopoulos D. Endocytosis of liposomes and intracellular fate of encapsulated molecules: encounter with a low pH compartment after internalization in coated vesicles. *Cell.* 1983;32:1069-1079.
48. Mayer LD, Bally MB, Cullis PR. Uptake of adriamycin into large unilamellar vesicles in response to a pH gradient. *Biochim Biophys Acta.* 1986;857:123-126.
49. Haran G, Cohen R, Bar LK, Barenholz Y. Transmembrane ammonium sulfate gradients in liposomes produce efficient and stable entrapment of amphipathic weak bases. *Biochim Biophys Acta.* 1993;1151:201-215.
50. Allen T, Chonn A. Large unilamellar liposomes with low uptake into the reticuloendothelial system. *FEBS Lett.* 1987;223:42-46.
51. Gabizon A, Papahadjopoulos D. Liposome formulations with prolonged circulation time in blood and enhanced uptake by tumors. *Proc Natl Acad Sci U S A.* 1988;85:6949-6953.